Structural, Optical, and Electronic Properties of Silicon/Boron Phosphide Heterojunction Photoelectrodes

A. Goossens, E. M. Kelder, R. J. M. Beeren, C. J. G. Bartels, and J. Schoonman

Delft University of Technology, Laboratory for Inorganic Chemistry, Julianalaan 136, 2628 BL Delft, The Netherslands

Electrical Properties / Impedance Spectroscopy / Materials Properties / Photoelectrochemistry / Semiconductors

This paper presents structural, optical, and electronic properties of Si coated with a thin epitaxial layer of n-type BP, which serves as protective optical window. n-Si/n-BP, as well as p-Si/n-BP heterostructures have been grown by CVD and investigated. p-Si/n-BP heterojunction photo-electrodes produce large and stable photocurrents up to 15 mA/cm^2 when applied in liquid junction solar cells. The origin of this photocurrent is discussed. Impedance spectroscopy is used to obtain Mott-Schottky plots from which the flatband potential of crystalline boron phosphide is determined. The band structure of the heterojunction is shown to agree with the optical features. Finally, the distribution of the potential drop in the heterostructure is elucidated.

Introduction

The application of photo-electrochemical (PEC) cells in the conversion of solar energy into electrical energy or fuel has attracted widespread interest recently. Since Fujishima and Honda [1] reported on the successful utilization of TiO_2 semiconductor electrodes, much effort has been directed towards improvement of the PEC solar cell materials. A wide variety of semiconductor electrode materials have been investigated thoroughly and detailed information about the physics and chemistry of semiconductor/electrolyte (sc/el) interfaces has become available.

In general there are three major drawbacks which prevent the successful conversion of solar energy employing PEC cell configurations. Firstly, the semiconductors that are known to be photochemically stable all have a bandgap of 3 eV or larger. However, as the maximum of the solar spectrum lies at about 1.4 eV, these semiconductors are not sensitive for a substantial part of the solar spectrum. Consequently PEC cells based on the photosensitivity of these materials can operate only with very low efficiencies. Secondly, semiconductors that do have a suitable bandgap of about 1.4 eV are known to be (photo)-chemically unstable. This instability is caused predominantly by the presence of electron holes at the sc/el interface. If the valence band comprises bonding orbitals, as is frequently the case, the presence of holes at the sc/el interface offers species in the electrolyte the opportunity to form chemical bonds with atoms on the semiconductor surface. When a semiconductor surface atom has formed one or more of such bonds it is thermodynamically unstable and may eventually be solvated. In several instances, like Si, however, an insoluble and insulating oxide layer is formed rapidly. In p-type materials an appreciable number of holes is present at the sc/el interface if the electrode is either in the dark or illuminated. In n-type materials holes are absent in the dark, but are generated upon irradiation, and subsequently drift towards the surface when depletion exists. Thirdly, many electrolytes with fast electron kinetics are known to be photochemically active. In addition to absorption of solar radiation, a concomitant photochemical dissociation reaction may occur if the electrolyte is irradiated strongly.

In order to overcome the first and second drawbacks, the utilization of heterojunction electrodes has been proposed. If a wide bandgap semiconductor is deposited onto a small bandgap substrate it may serve as a protective optical window. Both the efficiency as well as the stability can be optimized in such configurations. Especially metal oxides were investigated as wide bandgap optical windows [2–4].

In Fig. 1 the large bandgap oxides that have been discussed in the Ref. [5–13] as protective window materials on Si photoelectrodes are listed along with their conduction band and valence band energies. The conduction and valence band energy of silicon is taken from the Ref. [11, 14–16]. As can be seen easily from this figure, the valence band energies of the oxides, with the possible exception of Fe_2O_3, are found far below the valence band energy of silicon. Hence, when n-type Si is to be used as a photoanode, the optically generated holes in n-Si are unable to drift into the valence bands of any of these oxides. The only alternative way for holes to cross the Si/oxide junction is recombination with electrons from the conduction band of the oxide. This process leaves a "hole" in the conduction band of the oxide that can subsequently be transported towards the electrolyte. This conduction mechanism can occur only when an

  0005-9021/91/0404-0503 $ 3.50+.25/0

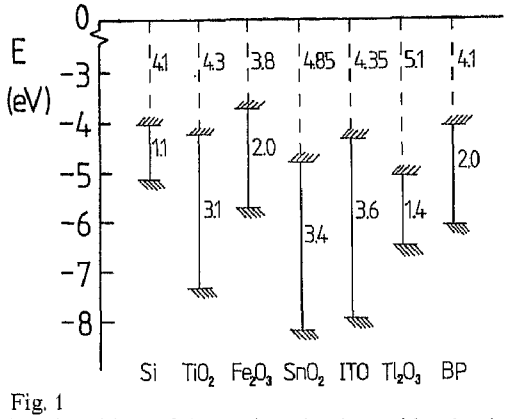

Fig. 1
Band positions of the semiconducting oxides that have been applied as protective window material for silicon photoelectrodes. ITO is an abbreviation for Indium-Tin Oxide. The zero energy level is defined at vacuum and the H^+/H_2 redox potential lies 4.5 eV below the vacuum level

n-type window material is applied. The oxidative potential of the photoholes is only preserved if the conduction band of the oxide lies close to the valence band of the substrate. If these conditions are fulfilled the heterojunction is called type A [11]. Using n-Si as a substrate, the best type A heterojunction photoelectrodes are n-Si/n-SnO_2 and n-Si/n-Tl_2O_3.

When p-Si is used as a photocathode, the photoelectrons in the conduction band of Si are able to cross the Si/oxide interface in two ways. They can recombine with holes from the valence band of the oxide. In this recombination process, however, the photoelectrons lose all of their reductive potential. For this mechanism a p-type window material is required. Alternatively the photoelectrons can drift into the conduction band of the n-type oxide. In order to preserve their optical excitation energy, a good match between the conduction band of the substrate and the conduction band of the window is required. These heterojunctions are denoted type B [11]. From Fig. 1 it can be seen that with n-TiO_2, n-ITO (indium tin oxide), and with the presently studied epitaxial boron phosphide window material n-BP, the most promising type B heterojunction photoelectrodes based on Si substrates can be formed.

Ginley, Baughman, and Butler [17] proposed the utilization of degenerate mono-crystalline n-type BP as window material on n-type Si and n-type GaAs electrodes. Their device basically resembled a metal coated semiconductor electrode. Hence, the band bending in the substrate material is in principle determined entirely by the work function of the coating material, while the electrolyte only serves as an electrical contact between the counter electrode and the "metal" coated photoelectrode. They showed that the n-Si/n-BP system was stable in a ferri-ferrocyanide redox couple. More than 10^4 Q charge could be passed through their PEC cells without a significant loss of the efficiency of the cell. While the importance of a good bandmatch was recognized, these authors failed to determine the flatband potential of BP experimentally. The position of the conduction and valence bands of BP were calculated from their semi-empirical electronegativity model [18, 19]. In the band diagram which was derived from these calculations, the conduction bands of Si and BP are at about the same energy level. Hence, a small band bending in the Si substrate must be expected for n-Si/n-BP structures. The photoholes which are generated in Si are unable to drift into the valence band of BP, and instead recombine at the Si/BP junction with electrons from the conduction band of BP. Therefore, the electrical charge is carried through the BP window towards the electrolyte by its majority carriers, i.e. conduction band electrons instead of (photo) holes. The recombination process at the Si/BP junction converts the exitation energy of the photohole into heat and decreases the efficiency of the cell dramatically.

Here we present structural, optical, and electronic properties of crystalline non-degenerate n-type boron phosphide protective optical windows on silicon photoelectrodes. Both n-Si/n-BP, and p-Si/n-BP heterojunction configurations have been investigated. The photoelectrochemical properties of polycrystalline BP were elucidated in our previous study [20]. In the work of Lee at al. crystalline p-type BP is employed as photocathode [21].

Scanning Electron Microscopy (SEM), X-ray diffraction (XRD), and Auger depth profiling are used to determine the crystal structure and the stoichiometry of the composite. The spectral photocurrent response of both configurations n-Si/n-BP and p-Si/n-BP is recorded from which the quantum yield spectra could be derived. Impedance spectroscopy is used to determine the space charge capacitance of BP at depletion. the Mott-Schottky plot of C^{-2} versus the d.c. bias provided the donor density of the BP layers and the flatband potential of boron phosphide, the latter parameter being of fundamental importance in the description of sc/el interfaces. The quantum yield spectra, and the Mott-Schottky behavior of the space charge capacitance provides coherent information about the band structure of the heterojunction. Moreover, the potential distribution in this electrode could be derived from the impedance data. Chemical information about the sc/el interface is obtained by variation of the pH of indifferent electrolytes, as well as, from the PEC cell's photoresponse in electrolytes with active redox species.

Only when the p-Si/n-BP configurations is used light energy can be converted at current densities of 15 mA cm^{-2} without deterioration of the cell characteristics for more than 1000 hours of continuous operation.

Experimental Aspects

Epitaxial layers of BP on Si substrates were obtained by Chemical Vapor Deposition (CVD) using a cold wall reactor [22]. The silicon substrates used were in all cases (100) oriented with resistivities of about 0.1 Ω cm. The n-type Si substrates were doped with phosphorus to a donor density (N_D) of 10^{17} cm^{-3}. The p-type Si substrates were doped with boron to an acceptor density (N_A) of also 10^{17} cm^{-3}. Prior to deposition the silicon wafers were cleaned in acetone followed by an ultrasonic etch in ultra pure 100% HNO_3 for 30 minutes. Finally, a 1 minute dip in a 5% HF solution was applied to remove the SiO_2 surface layer. Between every step the Si wafers were rinsed thoroughly with distilled water. Finally, the small water drops on the Si surface were removed by spinning the

Si pieces under a flow of ultra dry methanol. Immediately after the HF dip, the water rinse, and the methanol spin-drying, the wafers were placed in the furnace which was evacuated, and subsequently filled with purified hydrogen.

Prior to every deposition the carbon susceptor was etched under a 5% HCl/95% H_2 gas mixture at a temperature of 1100°C. This etching procedure was necessary in order to remove the previously deposited BP from the susceptor.

The carbon susceptor was heated inductively to about 900°C during the deposition. Evaporated BBr_3 and PBr_3 reactants were diluted with oxygen free and dry hydrogen and fed into the furnace in a molecular ratio of 1 to 20. A growth rate of typically 1 to 2 μm per hour has been achieved. Details on the CVD procedure have been published earlier [23].

After chemical cleaning, an ohmic contact of aluminum was provided at the back of the Si electrode which was subsequently sealed onto a PVC holder and brought into a teflon three electrode photoelectrochemical cell. A large area Pt sheet (≈40 cm^2) was used as counter electrode, and a saturated calomel electrode (SCE) served as the potential reference. As indifferent aqueous electrolytes H_2SO_4 (0.5 M), buffered KCl (1 M) (with NaAc/HAc (0.02 M)), and KOH (1 M) were used.

The electrode could be irradiated through a quartz window. A 250 W tungsten-halogen lamp, and a 450 W high pressure Xe lamp (OSRAM XBO 450 W) were used as light sources. A Zeiss MM12 double prism monochromator and a Bausch & Lomb high intensity grating monochromator were used in combination with Schott high-pass filter glasses to measure the spectral photocurrent responses. The complete optical system: lamp, condenser, monochromator, high-pass filter glasses, positive focusing lens, and the quartz optical window was calibrated with a Kipp & Zonen compensated thermopile CA1. With this instrument, the photon flux at every wavelength can be obtained and this flux can be used to scale the spectral photocurrent of the cell.

The $i-V$ characteristics in the dark and under illumination were recorded at low scan rates, i.e. <1 mV/s, with an Electrochemical Interface (Solartron ECI 1286) coupled to a plotter. In order to be able to observe the small current response on monochromatic irradiation, the light beam was mechanically chopped at 12 Hz, amplified by the potentiostat, and recorded with an EG&G/PAR dual Lock-In Amplifier (model 5210).

The impedance was recorded at 40 different frequencies between 10 Hz and 65 KHz (10 frequencies per decade) using a Frequency Response Analyzer (Solartron FRA 1260) coupled to the Electrochemical Interface (ECI 1286). A 10 mV amplitude sinusoidal voltage stimulus was superimposed on the potentiostatically controlled d.c. bias, and the current response was detected. The d.c. bias was stepped through the desired potential region and an impedance spectrum was recorded at the end of every step interval. The bias intervals were 50 mV and a staibilization time of 500 s was maintained before an impedance spectrum was recorded. The impedance spectra were recorded fully automatically by control with a personal computer.

Results

The Electrode Composition

Chemical Vapor Deposition in a cold wall reactor with inductive substrate heating and BBr_3 and PBr_3 as reactants is a suitable method to obtain thin monocrystalline n-type BP layers on Si substrates. When (100) Si is used, the crystallographic orientation is preserved in the BP coating, i.e. epitaxial layers are formed. X-Ray Diffraction (XRD) confirms the top layer to be mono-crystalline BP and its orientation to be (100). A twinning in the epitaxial BP layers is observed. Infrared transmission spectra with the radiation crossing the Si as well as the BP, reveals the characteristic fundamental optical phonon absorption of crystalline BP at 827 cm^{-1} [24]. For all samples this characteristic infrared absorption was observed.

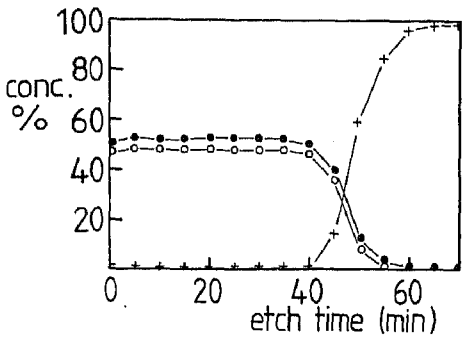

Fig. 2
Auger depth profile of a Si/BP heterostructure ●●● denotes phosphorus, ○○○ denotes boron, and + + + denotes silicon

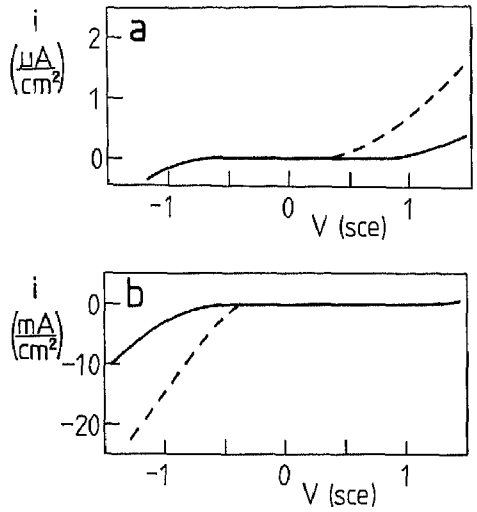

Fig. 3
i-V characteristics of n-Si/n-BP photoanodes (a) and p-Si/n-BP photocathodes (b) ——— = dark current (i_d), – – – = dark plus photocurrent ($i_d + i_{ph}$)

Auger profiling provided insight into the distribution of the elements in the laminar composite. In Fig. 2 the depth profile of a Si/BP heterojunction is presented. The interfacial region is sharp, and the stoichiometry in the bulk of either Si or BP is well defined.

The spectral photocurrent response

When the electrode is irradiated with tungsten-halogen light, 100 mW cm^{-2}, and the potential sweeped slowly, 1 mV/s, from +1.5 to −1.5 V vs. SCE, a photocurrent is observed. For n-Si/n-BP heterojunctions an anodic photocurrent in the μA cm^{-2} range sets in at +0.3 Volt versus SCE. For p-Si/n-BP electrodes large cathodic photocurrents in the mA cm^{-2} range are observed for voltages more negative than −0.4 Volt. Here H_2SO_4 (1M) is used as electrolyte. In Fig. 3a,b the dark current (i_d) and the summation of the dark and the photocurrent ($i_l = i_d + i_{ph}$) are plotted as a function of the electrode potential for both studied configurations.

The excitation spectrum of the photogenerated minority carriers was detected by recording the photocurrent at a fixed potential. For n-Si/n-BP the polarization was +1 V, and for p-Si/n-BP electrodes, −1 V vs. SCE was used. In this experiment a completely different behavior is observed for the two studied configurations. n-Si/n-BP electrodes reveal an anodic photocurrent that was generated by photons with $h\nu > 2.0$ eV. p-Si/n-BP electrodes show a cathodic photocurrent generated by photons with $h\nu > 1.1$ eV. The excitation spectra of the two studied configurations are presented in Fig. 4a,b. In this figure the current response is divided by the

irradiation flux to obtain the quantum yield (QY). The quantum yield is plotted as a function of the incident photon energy (E_{ph}). It should be noted that the fixed potentials at which these spectra were recorded are not corresponding with the maximum of the photocurrent response. By choosing a d.c. potential at which the dark current and the photocurrent are still low, problems due to diffusion limitations of species in the electrolyte and problems due to extensive H_2 or O_2 formation at the electrode surface, which disturbs the measurements severely, could be avoided.

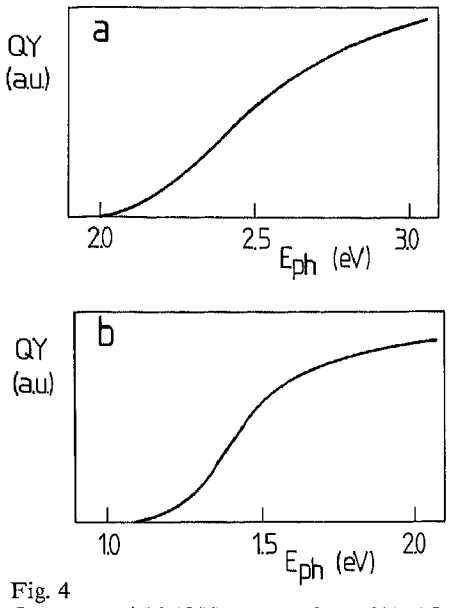

Fig. 4
Quantum yield (QY) spectra for n-Si/n-BP (a), and for p-Si/n-BP (b) configurations

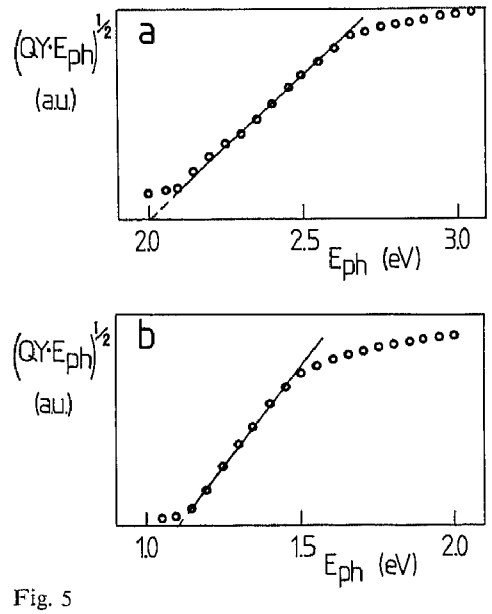

Fig. 5
Determination of the bandgap of BP in n-Si/n-BP electrodes (a), and of the bandgap of Si in p-Si/n-BP electrodes (b) from the quantum yield spectra

The optical bandgap can be obtained from a plot of $(QY \cdot E_{ph})^{\alpha}$ as a function of E_{ph}. For direct transitions, α reads 2 and for indirect, i.e. phonon assisted transitions, α reads 1/2 [25]. As shown in Fig. 5a,b, a linear region is found for both electrode configurations when for α the value 1/2 is chosen. The linear region extrapolates to an intercept with the energy axis of 2.0 eV for the case of n-Si/n-BP, and 1.1 eV in case of p-Si/n-BP.

The Flatband Potential of Boron Phosphide

To determine the positions of the conduction band and the valence band of BP, impedance spectra at different d.c. electrode potentials were recorded. In order to obtain impedance data from the window material only, the interface between Si and BP was shunted. Two Al ohmic contacts were provided symmetrically on the surface of the BP window by thermal evaporation at 10^{-6} mbar pressure. After a subsequent anneal at 450°C for 30 minutes, a gold layer was sputtered on the Al and on the back side of the Si. The gold layers made contact and hence shunted the Si/BP interfacial region. In Fig. 6a the electrode configuration is presented.

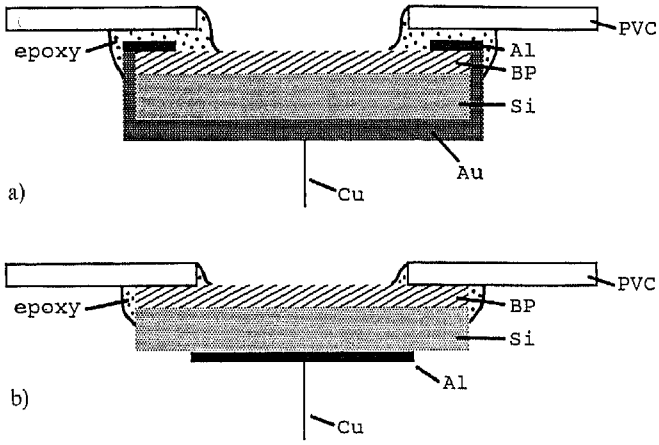

Fig. 6
The electrode configuration with a shunted substrate (a) and with the electrical path through the complete heterojunction (b)

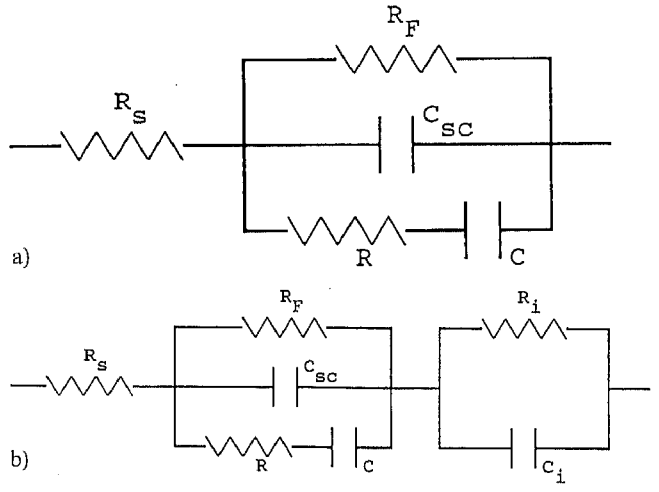

Fig. 7
The equivalent circuits used to model the impedance of shunted substrate electrodes (a) and the impedance of heterostructure electrodes (b)

The impedance spectra were recorded in the indifferent electrolytes, H_2SO_4 (0,5 M), KCl (1 M) + HAc (0.02 M) + NaAc (0.02 M), and KOH (1 M). The impedance spectra of the shunted substrate electrodes could be fitted to a simple equivalent circuit comprising an ohmic loss resistance, R_s, coupled in series to a parallel combination of a Faradaic charge transfer resistance R_F, the space charge capacitance C_{sc}, and a series RC surface recombination

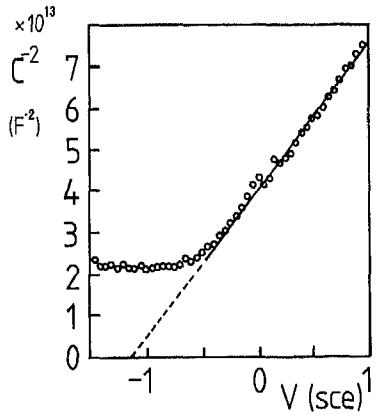

Fig. 8
Mott-Schottky plot of C^{-2} versus electrode potential for a shunted substrate electrode recorded in the dark with KOH (1 M) as electrolyte. When measured through the complete heterojunction, identical MS-plots were obtained. The surface area of the electrodes was 7 mm^2

branch. Fig. 7a depicts this equivalent circuit. For a few samples the accuracy of the fit could be improved by using the non-Debye "*Q*-element" in stead of a true space charge capacitance. The impedance of this element is $Z_Q = Q^{-1}(j\omega)^{-\alpha}$. The value of α was in all cases larger than 0.9 which makes it is permissible to regard the *Q*-element as a slightly disturbed capacitance. The used non-linear least squares fitting program, "Equivalent Circuit" was developed by Dr. B. Boukamp at the Technical University of Twente in The Netherlands and kindly put at our disposal. From the C_{sc} values as a function of bias, the Mott-Schottky (MS) plots of $(C_{sc})^{-2}$ versus d.c. bias, *V*, were constructed. As shown in Fig. 8, linear MS-plots were obtained. The applied experimental technique does not allow a frequency dependence in any of the circuit elements. The extrapolated bias intercept, V_0, was identical for both electrode configurations and read $-0.55+/-0.05$V vs. SCE in the buffered KCl electrolyte. The potential axis intercept is observed to shift $-60+/-5$ mV at unit pH increment over the full pH range of 0 to 14. The slope of the MS-plot was positive concordant with an effective donor density $N_D - N_A$ of about $5 \cdot 10^{19}$ cm^{-3} for all studied samples.

Impedance spectra were also recorded through the complete heterojunction. As shown in Fig. 6b an ohmic contact was provided on the back side of the Si in these experiments. The equivalent circuit that could be used to model the small signal a.c. response of the system n-Si/n-BP heterojunction photoelectrodes in indifferent electrolytes was similar to the equivalent circuit of the shunted substrates extended with an additional parallel RC network. In Fig. 7b this equivalent circuit is presented. Despite of the complexity of this equivalent circuit, one of the capacitances could be related to the space charge capacitance of BP at the BP/electrolyte interface. Also for this heterostructure linear and frequency independent Mott-Schottky plots were obtained in KCl and KOH electrolytes. From the slopes an effective donor density $N_D - N_A$ of about 5×10^{19} cm^{-3} was derived, which is in agreement with the value found in the shunted substrate experiments. The potential axis intercept V_0 was identical to the Mott-Schottky intercept as found in the previously described experiments on the shunted substrates. The elements of the additional *RC* network, R_i and C_i were observed to be nearly independent of the applied d.c. bias. R_i was about 5 Ω cm^2 and C_i varied between 0.2 to 0.3 μF cm^{-2} for the different studied samples.

The Stabilization Efficacy

In order to determine the protective efficacy of the thin BP windows, a p-Si/n-BP sample was placed in a H_2SO_4 (1 M) electrolyte, biased with -2 V (no reference electrode was used), and irradiated with 100 mW cm^{-2} tungsten-halogen light. A bias of -2 V corresponds with an electrode potential of approximately -1.5 V vs. SCE. A photocurrent of about 10 mA cm^{-2} was observed. This photocurrent was stable over 1000 hours of continuous operation. After this period the experiment was terminated. The BP surface that had contacted the electrolyte had a black, somewhat rough appearance. With Scanning Electron Microscopy the presence of a rough surface layer was observed indeed. X-ray diffraction unambiguously characterized this surface layer to be polycrystalline hexagonal B_2O_3. It must be noted that during the 1000 hours of operation the photocurrent was stable, or in fact showed even a slight tendency to increase. Hence the B_2O_3 layer is probably both transparent and conducting.

Discussion

Epitaxi of BP on Si

Epitaxial layers of BP can be grown on (100) Si substrates by CVD. The large difference between the lattice parameters of Si and BP, together with the difference in thermal expansion induces stress in the interfacial region. This stress, however, is relaxed by twinning of the BP lattice in a small interfacial region [26]. Both the crystallographic orientation as the twinning is observed by XRD.

Despite the high deposition temperature of about 900°C, the diffusion of Si into the BP layer, and of B or P into the Si substrate is limited to a small (nanometer) interfacial region.

The Spectral Photocurrent Response

Heterojunction electrodes comprising n-Si/n-BP produce small anodic photocurrents when irradiated with high energetic photons, i.e. $E_{ph} > 2{,}0$ eV. Obviously this photocurrent is generated only in the window material n-BP and not in the n-Si substrate. Apparently holes created in the Si are unable to reach the BP/electrolyte interface. Hence annihilation of the photoholes by conduction band electrons of Si must occur at the n-Si/n-BP interface.

Configurations comprising p-Si/n-BP electrodes produce large cathodic photocurrents when irradiated with low energetic photons, i.e. $E_{ph} > 1.1$ eV. Here the photogenerated electrons in Si do cross the Si/BP interface and reach the electrolyte to drive a reduction reaction there. For $E_{ph} > 2.0$ eV, photoholes are generated in BP in addition to the photoelectrons in Si. The photoholes in BP, however, are so few in number with respect to the numerous conduction band electrons, that recombination is likely to take place before they reach the electrolyte.

The band structure of the Si/BP heterojunction prevents Si holes to cross the SI/BP junction, but does make it possible for conduction band electrons of Si to cross the window and reach the electrolyte.

The Flatband Potential and the Barrier Height of the Si/BP Junction

From MS-plots the energy band structure of a semiconductor can be elucidated. The flatband potential (V_{fb}) is related to the intercept of linear MS-plots with the potential axis (V_0). If the Helmholtz capacitance is large with respect

to the space charge capacitance, and if abundant charge accumulation in surface states is absent; $V_{fb} = V_0 - kT/e$ [27]. For crystalline CVD layers of (100) oriented BP, the flatband potential reads -0.55 V vs. SCE at pH = 4.6, and is observed to show a Nernstian -60 mV/pH dependence. The point of zero charge (PZC) of BP was determined with the method proposed by Ginley et al. [28], and lies at pH = 6.4. The energy difference between the conduction band of n-BP and the Fermi level was determined from the thermoelectric behavior of n-BP and was found to be about 0.05 eV [29]. Hence, the energy of the conduction band and the valence band of crystalline BP is determined on the absolute energy scale, i.e., versus vacuum.

E_c(BP) = $(+0.32 + 0.06 \cdot \text{pH})$ eV vs. SCE

E_v(BP) = $(-1.68 + 0.06 \cdot \text{pH})$ eV vs. SCE

Experimental accuracy $\approx$ 0.05 eV

PZC (BP) lies at pH = 6.4

SCE $\approx$ 4.75 eV below vacuum level

The position of the conduction and valence band of rough polycrystalline BP layers is determined in our previous study [20]. Only a relative small difference of 0.26 eV between the bands of the presently studied crystalline BP and the polycrystalline samples of our previous study appears to exist.

Silicon is known to have a conduction band energy of about + 0.7 eV vs. SCE and a valence band at -0.4 eV vs. SCE. Therefore, the conduction band of Si matches excellently with the conduction band of BP allowing conduction band electrons to pass easily through the Si/BP junction. However, the valence bands of Si and BP differ considerably. Valence band holes in Si faces a 0.9 eV potential barrier at the Si/BP junction and recombine with electrons instead of crossing. In Fig. 9 the band structures of the n-Si/n-BP, and p-Si/n-BP heterojunction configurations are presented. In this Fig. Anderson's approach [30], in which the band bending at the heterojunction interface is simply derived from the bulk properties of both materials, is followed.

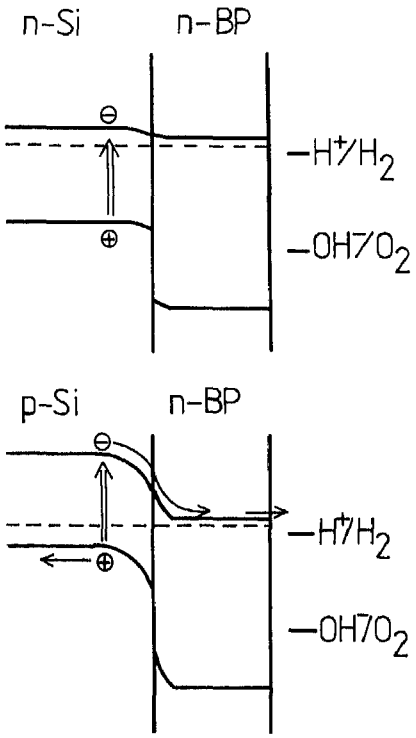

Fig. 9
Band structure of n-Si/n-BP and p-Si/n-BP heterojunction photoelectrodes. The redox potentials of H^+/H_2 and OH^-/O_2 are 4.5 respectively 5.73 eV below vacuum level

The Potential Distribution

When measured through the heterojunction device, the space charge capacitance of BP at the BP/electrolyte junction is observed to have the same potential dependence as measured with front contacts on the BP window, and a shunted Si substrate. Also no differences were detected between the Mott-Schottky behavior of either n-Si/n-BP or p-Si/n-BP heterojunctions. Apparently the externally applied potential difference falls across the depletion region of BP at the BP/electrolyte interface, and not across any other region in the heterojunction electrode. This is especially true for the Si/BP interfacial region. Externally applied potentials do not drop at the Si/BP interfacial region, and hence do not influence the band bending of Si or BP there. In unilluminated heterojunction electrodes the electrons are in equilibrium at every cell potential. In other words, the Fermi level lies at the same energy level (is horizontal) throughout the heterojunction photoelectrode at given electrode potential. When the electrode potential is changed by means of an externally applied potential or by addition of a redox couple to the electrolyte, an additional electric field is created in the space charge region of BP at the BP/electrolyte interface. The electric field at the Si/BP junction, however, is not influenced by external applied potential differences. In Fig. 10 the influence of an externally applied bias on the band bending in a BP window on Si substrates is presented.

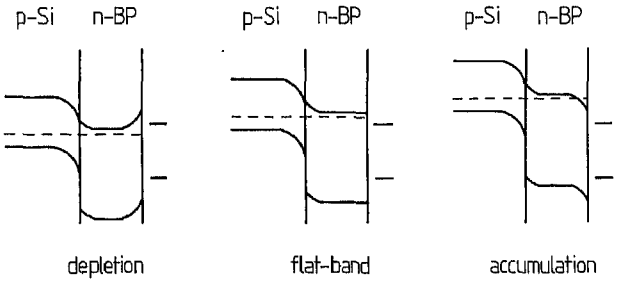

Fig. 10
The influence of an externally applied potential on the band bending in p-Si/n-BP electrodes. Depletion at an anodic bias, the flatband situation, and accumulation at cathodic bias

The extension in the equivalent circuit which occur when measured through the heterostructure must be attributed to the Si/BP interface. Since R_i is much smaller than R_F, the quantitative accuracy of the fit results is rather poor for both

R_i and C_i. Despite of this, however, our notion that the potential drop occurs primarily at the BP/electrolyte interface is supported by the observation of the parallel $R_i \cdot C_i$ circuit. The d.c. potential drop is distributed as follows: a portion $R_F/(R_F + R_i)$ falls across the depletion layer in BP at the BP/electrolyte interface, and a portion $R_i/(R_F + R_i)$ across the Si/BP junction. Although R_F depends strongly on the electrode potential, it never reduces below 1 K Ω cm^{-2}, while R_i reads about 5 Ω cm^{-2}. Consequently, the portion of the potential drop that occurs at the Si/BP interface is negligible for every electrode potential. As a result of this C_i, being the space charge capacitance of Si, is unaffected by an externally applied bias. Its magnitude is fixed, and so is the band bending of Si. The constant value of C_i corresponds with a constant bending of the bands in Si at the Si/BP interface of 0.5+/−0.2 Volt.

Photoelectrochemical Energy Conversion with Si/BP Electrodes

From the durability test of p-Si/n-BP photoelectrodes in H_2SO_4 it is observed that this electrode sustains large photocurrents even at unfavorable circumstances such as high irradiation intensities, large cathodic bias, and an indifferent electrolyte. During the full test more than 30,000 Q cm^{-2} charge passed through the device which means that for every atom present in the thin coating, B or P, more than 40,000 electrons crossed the window. Obviously the device is extremely stable with regard to the photocurrent for photocathodic processes in H_2SO_4.

The observation that a polycrystalline hexagonal B_2O_3 layer is formed on the BP surface in acidic electrolytes needs further investigation. We assume that phoshorus is reduced at the surface and solvates as a phosphate. The formation of B_2O_3 finally prevents the continuation of this process because it inhibits phoshorus diffusion. Consequently the degradation of the surface stops after the formation of a certain amount of B_2O_3. The mechanism of the formation of B_2O_3 is presently under study.

The p-Si/n-BP electrode must be biased negative vs. SCE in order to reduce the band bending in BP. Only when the potential barrier for the conduction band electrons in BP is absent or small, a cathodic reduction reaction can occur. This necessary negative bias can be provided by a suitable redox electrolyte. A redox couple of V^{2+}/V^{3+} was prepared following the description of Heller et al. [31]. The redox potential was −0.35 V vs. SCE at properly de-airated electrolytes. Despite the large optical absorption of this electrolyte, a maximum short circuit photocurrent, i_{sc}, of 15 mA cm^{-2} could be reached with 80 mW cm^{-2} irradiation power. The open circuit potential, V_{oc}, was about 0.5 V and the fill factor, η, about 0.5. The maximal gained power at 80 mW cm^{-2} irradiation power equals $(V \times i)_{max} = \eta(V_{oc} + i_{sc}) =$ 3.75 mW cm^{-2} which yields a conversion efficiency of tungsten-halogen light of 4 to 5%.

In this heterojunction liquid junction solar cell the cathodic photocurrent is generated in the p-type Si substrate and is involved in the reduction of V^{3+}, i.e. $V^{3+} + e^- \rightarrow V^{2+}$, at the BP/electrolyte interface. The open circuit potential is determined by the band bending in Si and not by the band bending in BP. The former is determined by the difference in the Fermi level between p-Si and n-BP which amounts to about 0.8 V. The latter, however, is determined by the difference between the Fermi level in n-BP and the redox potential of the V^{2+}/V^{3+} couple. This couple has a redox potential of about −0.35 V vs. SCE which is equal to the Fermi level in n-BP. Consequently, the band bending of n-BP is about zero in a V^{2+}/V^{3+} couple.

Conclusions

The utilization of large bandgap semiconductors as protective optical windows on small bandgap photoelectrodes can stabilize the PEC-cell's performance satisfactory. In order to achieve an efficient solar cell, the following four conditions must be fulfilled in such configurations.

(a) In order to be optically transparent, the window material must possess a significantly larger bandgap than the substrate semiconductor. (b) The window material must have a high conductivity in order to avoid ohmic losses in the cell. (c) If the substrate material is chosen to be p-type and the window material to be n-type (type B electrodes), holes are never present at the sc/el interface which ensures a durable cell operation. In the dark the n-type window inhibits the holes from the p-substrate to flow towards the surface. Upon irradiation, the minority photoholes from the window are annihilated by the photoelectrons from the substrate. (d) A p-substrate/n-window configuration can only be conductive for the photo-electrons if a good bandmatch between the conduction bands of the two materials is present.

All four requirements are fulfilled in a p-Si/n-BP heterojunction configuration. The externally applied potential drop falls across the depletion layer of BP at the BP/electrolyte interface. Hence a strong reductive electrolyte can by used to reduce the band bending in the BP window, and makes it possible for photoelectrons to drift into the liquid phase. Employing p-Si/n-BP heterojunction photoelectrodes in liquid junction solar cells can lead to durable and efficient solar energy conversion.

We are indebted to Ir. A. van den Assem for his experimental assistance in the CVD of epitaxial BP on Si substrates.

The investigations were supported by the Netherlands Foundation for Chemical Research (SON) with financial aid from the Netherlands Organization for Scientific Research (NWO).

References

[1] A. Fujishima and K. Honda, Nature *238*, 37 (1972).
[2] J. O'M Bockris and K. Uosaki, Energy *1*, 95 (1975).
[3] P. A. Kohl, S. N. Frank, and A. J. Bard, J. Electrochem. Soc. *124*, 225 (1977).
[4] M. Tomkiewicz and J. M. Woodall, J. Electrochem. Soc. *124*, 1436 (1977).
[5] H. P. Maruska and A. K. Ghosh, Sol. Energy Mater. *1*, 411 (1979).
[6] H. Morisaki, H. Ono, H. Dohkoski, and K. Yazawa, Jpn. J. Appl. Phys. *19*, L 148 (1980).
[7] T. Osaka, H. Kitayama, N. Hirota, and S. S. Eskilden, Electrochim. Acta *29*, 1365 (1984).

[8] T. Osaka, K. Ejiri, and N. Hirota, J. Electrochem. Soc. *131*, 1571 (1984).
[9] L. Thompson, J. DuBow, and K. Rajeshwar, J. Electrochem. Soc. *129*, 1934 (1982).
[10] G. Hodes, L. Thompson, J. DuBow, and K. Rajeshwar, J. Am. Chem. Soc. *105*, 324 (1983).
[11] F. Decker, J. Melsheimer, and H. Gerischer, Isr. J. Chem. *22*, 195 (1982).
[12] F. Decker, M. Fracastoro-Decker, W. Badawy, K. Doblhofer, and H. Gerischer, J. Electrochem. Soc. *130*, 2173 (1983).
[13] J. A. Switzer, J. Electrochem. Soc. *133*, 722 (1986).
[14] J.-N. Chazalviel, Surf. Sci. *88*, 204 (1979).
[15] Ph. Brondeel, M. Madou, W. P. Gomes, and F. Cardon, Sol. Energy Mater. *7*, 23 (1982).
[16] M. Madou, Ph. Brondeel, W. P. Gomes, P. Hanselaer, and F. Cardon, Sol. Energy Mater. *7*, 33 (1982).
[17] D. S. Ginley, R. J. Baughman, and M. A. Butler, J. Electrochem. Soc. *130*, 1999 (1983).
[18] M. A. Butler and D. S. Ginley, Chem. Phys. Lett. *47*, 319 (1977).
[19] M. A. Butler and D. S. Ginley, J. Electrochem. Soc. *125*, 228 (1978).
[20] A. Goossens, E.M. Kelder, and J. Schoonman, Ber. Bunsenges. Phys. Chem. *93*, 1109 (1989).
[21] J. Lee, A. Fujishima, K. Honda, Y. Kumashiro, Bull. Chem. Soc. Jpn. *58*, 2634 (1985).
[22] K. Shono, H. Othake, and J. Bloem, J. Cryst. Growth *45*, 187 (1978).
[23] E. M. Kelder, A. Goossens, P. J. van der Put, and J. Schoonman, J. Phys. *C5*, 567 (1989).
[24] S. Yugo, T. Kimura, Phys. Status Solidi (A) *59*, 363 (1980).
[25] T. S. Moss, G. J. Burrell, and B. Ellis, "Semiconductor Opto-Electronics", Butterworths, London 1973.
[26] Y. Hirai, K. Shono, J. Cryst. Growth. *41*, 124 (1977).
[27] W. P. Gomes and F. Cardon, Progr. Surf. Sci. *2*, 155 (1982).
[28] D. S. Ginley and M. A. Butler, J. Electrochem. Soc. *125*, 1968 (1978).
[29] E. M. Kelder, A. Goossens, and J. Schoonman, to be published.
[30] A. G. Milnes and D. L. Feucht, "Heterojunctions and Metal-Semiconductor Junctions", Academic Press, London, 1972.
[31] A. Heller, H. J. Leamy, B. Miller, and W. D. Johnston Jr., J. Phys. Chem. *87*, 3239 (1983).

(Received on September, 10th, 1990, E 7458
final version on December, 21st, 1990)